

Constrained composite Bayesian optimization for rational synthesis of polymeric particles

Fanjin Wang^{1,2,*}, Maryam Parhizkar², Anthony Harker³, Mohan Edirisinghe¹

¹Department of Mechanical Engineering, University College London, London, WC1E 7JE, United Kingdom

²School of Pharmacy, University College London, London, WC1N 1AX, United Kingdom

³Department of Physics and Astronomy, University College London, London, WC1E 6BT, United Kingdom

*Corresponding author, email: fanjin.wang.20@ucl.ac.uk

Abstract

Polymeric nano- and micro-scale particles have critical roles in tackling critical healthcare and energy challenges with their miniature characteristics. However, tailoring their synthesis process to meet specific design targets has traditionally depended on domain expertise and costly trial-and-errors. Recently, modeling strategies, particularly Bayesian optimization (BO), have been proposed to aid materials discovery for maximized/minimized properties. Coming from practical demands, this study for the first time integrates constrained and composite Bayesian optimization (CCBO) to perform efficient target value optimization under black-box feasibility constraints and limited data for laboratory experimentation. Using a synthetic problem that simulates electrospraying, a model nanomanufacturing process, CCBO strategically avoided infeasible conditions and efficiently optimized particle production towards predefined size targets, surpassing standard BO pipelines and providing decisions comparable to human experts. Further laboratory experiments validated CCBO's capability to guide the rational synthesis of poly(lactic-co-glycolic acid) (PLGA) particles with diameters of 300 nm and 3.0 μm *via* electrospraying. With minimal initial data and unknown experiment constraints, CCBO reached the design targets within 4 iterations. Overall, the CCBO approach presents a versatile and holistic optimization paradigm for next-generation target-driven particle synthesis empowered by artificial intelligence (AI).

Introduction

Polymeric micro- and nano-particles have received much attention in pharmaceuticals, catalysis, and energy applications due to their unique properties at a small scale^{1,2}. Diverse design requirements for particles, under the quality-by-design (QbD) framework, have been put forward by specific usages³. For example, particles as drug delivery platforms span diverse sizes across hundreds of nanometers by intravenous injection to micrometers for pulmonary administration⁴. However, the optimization of synthesis to meet these design requirements, within any manufacturing technology used, has mainly relied on human expertise and extensive trial-and-error experimentation.

Modeling strategies could facilitate the optimization of parameters towards design targets^{5,6}. Traditional design of experiment strategies can identify dominating factors in the processing parameters and direct towards optimal design, but the methodology poses limitations on the levels of variables that can be examined⁷. Supervised machine learning (ML) is powerful in modeling complicated relationships and serves well for predictive purposes⁸. However, the data-driven nature of these ML models have been related to have poor performance where available data are limited, which is often the case when the data are generated from laboratory-based experiments⁹.

Bayesian optimization (BO) was developed for efficient optimization of black box functions and scenarios where data acquisition is expensive^{10,11}. More recently, BO has emerged as a powerful tool for materials discovery purposes to find optimal materials properties¹²⁻¹⁴. However, two critical challenges were presented for the application of BO in targeted synthesis of materials. Traditional BO was developed to seek for a global maximum or minimum rather than matching a pre-defined target^{15,16}, whilst the latter has occurred as a common requirement in functional materials design. Another issue is associated with feasibility constraints in experimentation. Many current applications of BO within materials discovery and development^{14,17,18} did not incorporate feasibility. Nevertheless, practical concerns could emerge in BO recommendations due to a myriad of reasons in laboratory experiments, such as an impossible combination of material compositions, incompatible processing parameters, and limitations from apparatus. Shrinking the boundaries of variables in BO to a more practical region, or imposing known constraints to the optimization process^{19,20}, could mitigate the issue of generating infeasible experiments. It comes at the cost of sacrificing some of the search space and becomes impossible when the 'practical' region needs to be evaluated through experiments.

Here, we propose a combinatorial constrained composite Bayesian optimization (CCBO) pipeline showcasing efficient identification of suitable processing parameters in rational synthesis of polymeric particles. Through introducing a variational inference Gaussian process

(GP) component, the black box experiment feasibility was modeled and incorporated into BO acquisition function. Composite BO, on the other hand, handles the modeling of experimental parameters and targeting particle size through a composite objective function. Amongst various fabrication techniques of particles, electrospraying was selected as the model technique for its simplicity, versatility, and precision as a popular manufacturing method in drug delivery research²¹. It utilizes electric fields to deform the meniscus of polymer solution to form fine jets which eventually disintegrate into fine droplets. As these droplets travel towards a collector, they further shrink and solidify due to solvent evaporation. Processing parameters in electrospraying such as flow rate, voltage, polymer concentration, and the solvent could be adjusted to fine-tune the particle characteristics²². With CCBO, we demonstrate its superior performance in target parameter optimization compared with random baseline and conventional BO strategies through both synthetic data and wet-lab experiments of poly(lactic-co-glycolic acid) (PLGA) particles synthesis at multiple size targets.

Results

Validating CCBO through synthetic data. Performance of CCBO was first validated with synthetic experimental data. Before introducing the benchmark results, the configurations of the various BO pipelines tested in this study as controls are presented (**Fig. 1a**). More details of the implementation can be found in the method section. Briefly, the vanilla BO pipeline followed a traditional BO design where the target to be maximized was the negative squared distance y_{obj} . The feasibility component, which leveraged a variational GP for classification, was added to track experimental feasibility. Through factoring in a probability term into the acquisition function, the constrained BO pipeline was able to pick candidates with higher chance of success. Furthermore, CCBO adopted the same feasibility modelling, whilst modifying the objective component. It utilized GP to model the fundamental relationship in experiments between the processing variables \mathbf{x} with the size s . The negative squared distance function was incorporated in the acquisition function to prioritize candidates for minimizing the distance to the pre-set target. In terms of the synthetic problem, the data was produced by equations simulating electrospray processing. Specifically, the function for determining the size of electrosprayed particles (see equation (3)) was inspired by scaling laws proposed for electrospray and experimental observations, where flow rate and polymer concentration (through affecting the viscosity) are both positively correlated to the diameter with voltage having a negative impact^{22,23}. Logarithm and power transformations in the function were intended to add complexity in the modeling process to simulate the nonlinear nature of the electrospraying process. The constant for alpha was added to account for the impact of solvents considered in the process. Furthermore, the feasibility zone, as visualized in **Fig. 1b**, was set to be highly related to the flow rate and the solvent. The rationale was from practical

considerations where chloroform, as a highly volatile solvent, would result in clogged nozzle at lower flow rates. DMAc, at higher flow rates, would lead to insufficient evaporation of the solvent and produce splashes of droplets on the collector instead of solid particles.

As a benchmark, CCBO, together with random baseline, vanilla BO, and constrained BO only, were performed for 10 iterations. Five initial experiments were included, accounting for successful and failed cases for both solvents. The optimization target was set to 18 μm . Results for other target sizes, including 0.6, 3 and 6 μm , can be found in supplementary information (**Supplementary Fig. 1**). In each iteration, two sets of processing parameters were proposed and subjected to simulation functions to retrieve the synthetic experimental result as well as the feasibility. The regret, defined as the difference between the target and the closest candidate, was recorded after each iteration as a measurement of performance (**Fig. 1c**). After 10 iterations, the random baseline reached 0.8 μm regret. Similarly, the vanilla BO and constrained BO both achieved around 0.4 μm regret. By contrast, the CCBO algorithm rapidly converged to the targeted diameter after only two iterations.

To understand the recommendation process, the experiments proposed were visualized in **Fig. 1d**. The random baseline sampled uniformly across the experiment space with both solvents, resulting in many failed DMAc experiments due to the flow rate feasibility constraints. Vanilla BO started exploring the boundary conditions in the first few rounds. With an additional model to account for feasibility, the constrained BO algorithm managed to learn the feasible region for DMAc, as reflected by most DMAc experiments being recommended with lower flow rates. This corresponded well to the initial feasible zone visualized in **Fig. 1b**. In addition, the number of failed and successful attempts of each algorithm from the results in **Fig. 1e** were plotted, highlighting the reduction in infeasible experimental conditions with the help of the additional constraint model.

Furthermore, the CCBO strategy was observed to show highly efficient searching in a localized experiment space (**Fig. 1d**). This good performance of CCBO could be explained by its design. The routes taken by vanilla BO and constrained BO were directly minimizing the distance where the surrogate GP was forced to model more complicated results from both the experiment and the superimposed distance function. On the contrary, GP was solely used for modeling the black-box experiment results for CCBO. Our observations with CCBO echoed the findings in composite BO literature: extracting the analytically trackable part from the black box function can drastically benefit the optimization efficiency²⁴. In standard BO, the expected improvement (EI) acquisition function assumes Gaussian posterior distribution. However, the posterior of the composite function becomes non-Gaussian after the transformation with a non-linear function. To address this, Astudillo and Frazier suggested leaving the GP to model the black-box function.

With reparameterization trick, the composite part is instead incorporated in the acquisition function to transform the Gaussian posterior of the black-box function. This allows more efficient optimization through a closer approximation of posterior distribution in a composite scenario²⁵. In our implementation, the composite acquisition function was optimized in the CCBO pipeline with Monte Carlo sampling.

Finally, the model performance was compared to human users. Since the synthetic problem simulated the impact of experiment parameters, electrospaying users with a spectrum of experience were asked to compete against computational algorithms. They evaluated initial experimental data using their domain knowledge and suggested experiments to match towards a 3 μm target. The results were plotted on **Supplementary Fig. 2**. The CCBO strategy was behind an expert (10 years' experience) and an advanced user (5 years' experience) in the first iteration but soon overtook the advanced user in all following iterations. On the third iteration, the CCBO strategy managed to achieve a similar result to the expert. The intermediate user, however, lost the competition by sparing many chances to explore the higher flow rate region for DMAc. This might be due to user bias from previous experiments. Most interestingly, the beginner's luck brought our beginner user very close to an expert's performance in the first iteration. However, they failed to reach the target further due to lack of expertise in finetuning the processing parameters. Further visualization of the parameter selections revealed the preference of one-factor-at-a-time (OFAT) for expert and advanced users, as reflected by the linear patterns (**Supplementary Fig. 2c**). The intermediate and beginner users attempted to change multiple parameters in each iteration. In comparison, CCBO appeared to explore the region more strategically, minimizing regret (**Supplementary Fig. 2b**). It was thus argued that the CCBO algorithm could better explore the vast experiment space and offer comparable performance to that of experienced users with years of expertise. In addition, the performance differences in users with various expertise further proved the success of setting up a representative synthetic problem of electrospaying. These results had consolidated our confidence in proceeding to a laboratory validation.

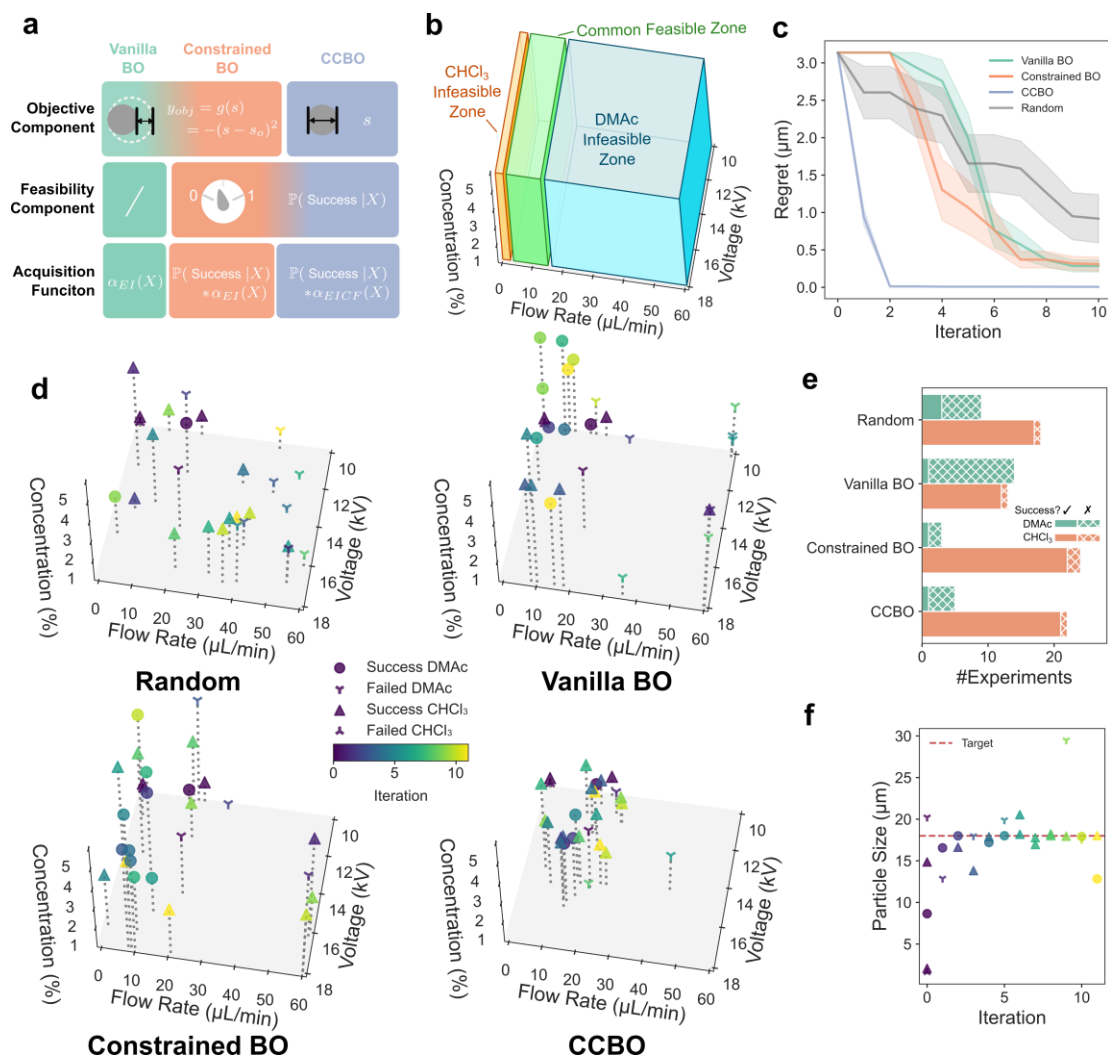


Fig. 1. Results for CCBO validation with synthetic data. **a** An illustration of configurations for vanilla BO, constrained BO, and CCBO. **b** Parameter space visualization for the synthetic data with feasibility zone highlighted for each solvent. **c** Benchmark results of target value optimization with random baseline, vanilla BO, constrained BO, and CCBO. The regret is calculated by the closest distance with respect to the design target, achieved at different iterations of BO. Each benchmark experiment was performed for 10 iterations. Shaded areas indicate standard error from 20 times repetition. **d** Visualization of experimental parameters suggested. Each data point represents one synthetic experiment. The corresponding iteration is coded by color. Symbols represent the solvent used and feasibility of experiment. **e** Comparison of total number of successful (filled bars) and failed experiments (hatched bars) in a typical run of 10 iterations with the four strategies. **f** The particle sizes produced with parameters chosen by CCBO. The iteration is color-coded to the data point and the symbols represent the solvent and feasibility. The target (18 μm) was highlighted as a dashed line.

Guiding laboratory electrospaying with CCBO for targeted particle production.

Following the validation of CCBO with synthetic data, it was applied in real-world experiments to guide electrospaying production of micro- and nanoparticles. The initial experiments,

generated through a Sobel sequence, were performed to accumulate foundational knowledge for BO pipelines (**Table 1**).

Table 1. Processing parameters generated through a Sobel sequence and the resulting particle sizes and feasibility (N=3).

Label	Polymer Concentration (% w/v)	Flow Rate ($\mu\text{L}/\text{min}$)	Voltage (kV)	Solvent	Mean Size (μm)	Feasible?
0-1	2.40	1.73	14.0	DMAc	0.56	1
0-2	4.06	0.44	15.7	CHCl_3	1.00	0
0-3	2.88	49.11	11.8	DMAc	15.00	0
0-4	0.76	0.01	17.6	CHCl_3	1.20	0
0-5	0.11	10.43	14.5	CHCl_3	6.26	1
0-6	3.55	0.06	12.8	DMAc	0.15	1
0-7	4.55	2.39	16.7	CHCl_3	5.24	1
0-8	1.88	0.21	11.0	DMAc	1.12	1

Two particle sizes, 300 nm and 3.0 μm , were set as the design targets based on pharmaceutical interests as drug carriers for intravenous injection and pulmonary delivery⁴. Based on previous reports, the production of PLGA particles with these two particle sizes require distinctive processing parameters involving different solvents and flow rates^{22,26}. Thus, the setting of these targets could simulate distinct typical experimental scenarios to challenge BO pipelines. The workflow of targeted particle production under CCBO guidance is illustrated in **Fig. 2a**. With the initial data gathered, CCBO pipeline was implemented to prompt two potential processing parameter sets for further laboratory experiments. After collecting samples and characterization, the results from triplicated experiments were evaluated and compared with the target. The next iteration of BO was performed based on the addition of the new data.

The proposed parameters by CCBO can be visualized with heatmaps in **Fig. 2b**. The heatmap of initial experiments reflected the diverse selections of parameters in Sobel sequence. In total, three iterations of BO were performed for the target of 300 nm and four iterations for 3.0 μm target. The selection of solvents was the most obvious difference for these two targets. Indeed, in previous reports of PLGA particle synthesis, DMAc was a popular solvent due to its high boiling point²⁷. From a mechanistic viewpoint, droplets will experience fission due to the competition between Coulombic repulsion and liquid surface tension in an electro spraying process²⁸. At the same time, the evaporation of solvents increases the concentration and viscosity of the droplet. As a non-volatile solvent, DMAc allows this fission process to fully develop and thus generates sub-micrometer particles²². Chloroform, on the contrary, was preferred in literature to produce larger particles within tens of micrometers range²⁹. These practical considerations, normally accumulated through experiences and trial-and-error, were

also picked up by the BO pipeline. The recommendations provided by CCBO clearly showed the trend of adopting DMAc for the 300 nm target and chloroform for the 3.0 μm target.

Linking the recommendations to the experiment results (**Fig. 2c**) could provide a more holistic viewpoint of the selection strategy of CCBO. For 300 nm target, the best candidate in initial experiments (0-8 on **Table 1**) used DMAc with a low polymer concentration, flow rate and voltage to obtain 0.15 μm particles. The recommendations from CCBO pipeline showed exploration of higher concentrations and fine-tuning of the flow rate parameter (**Supplementary Table 1**). Interestingly, the 3-1 and 3-2 experiments both achieved 300 nm particle size with distinct processing parameters, suggesting that the impact from less concentrated polymer solution was compensated by the higher flow rate used for 3-1. Furthermore, the balance of exploration-exploitation from the expectation improvement (EI) acquisition function was further demonstrated through the experiment series for 3.0 μm target. In the first iteration, CCBO attempted both DMAc and chloroform as the solvent (**Table S2**). The second iteration tested the lowest polymer concentration (0.05% w/v), which was shown as the lightest green in the heatmap (**Fig. 2b**). Finally, the recommendation settled down at higher concentration with reduced flow rates to approach the target with fine-tuning from exploitation. It was also observed from the SEM images (**Fig. 2d**) that the experiment 1-2 for 3.0 μm target managed to produce 2.69 μm particles with rough and polydisperse characteristic from a low polymer concentration (0.36% w/v) sprayed at a high flow rate of 3.65 $\mu\text{L}/\text{min}$. The final experiments 4-2 suggested 4.02% w/v solution sprayed at 1.08 $\mu\text{L}/\text{min}$ (**Supplementary Table 2**) to obtain 3.29 μm diameter particles. This result again highlighted the ability to achieve similar particle size through balancing polymer concentration and flow rate, together with adjusting other parameters. The SEM images of the final iteration experiments have shown satisfactory particle production at targeting sizes.

Overall, we have demonstrated superior performance of CCBO in the automatic identification of the experiment feasibility region and the rapid convergence to design targets through synthetic data validation. The comparison with human experts demonstrated CCBO's competitive performance. The rational exploration of experiment space outperformed the instinct-driven OFAT trial and error by humans. The wet-lab experiments, as a further step, consolidated CCBO's potential in real-world applications for guided particle synthesis within a few iterations.

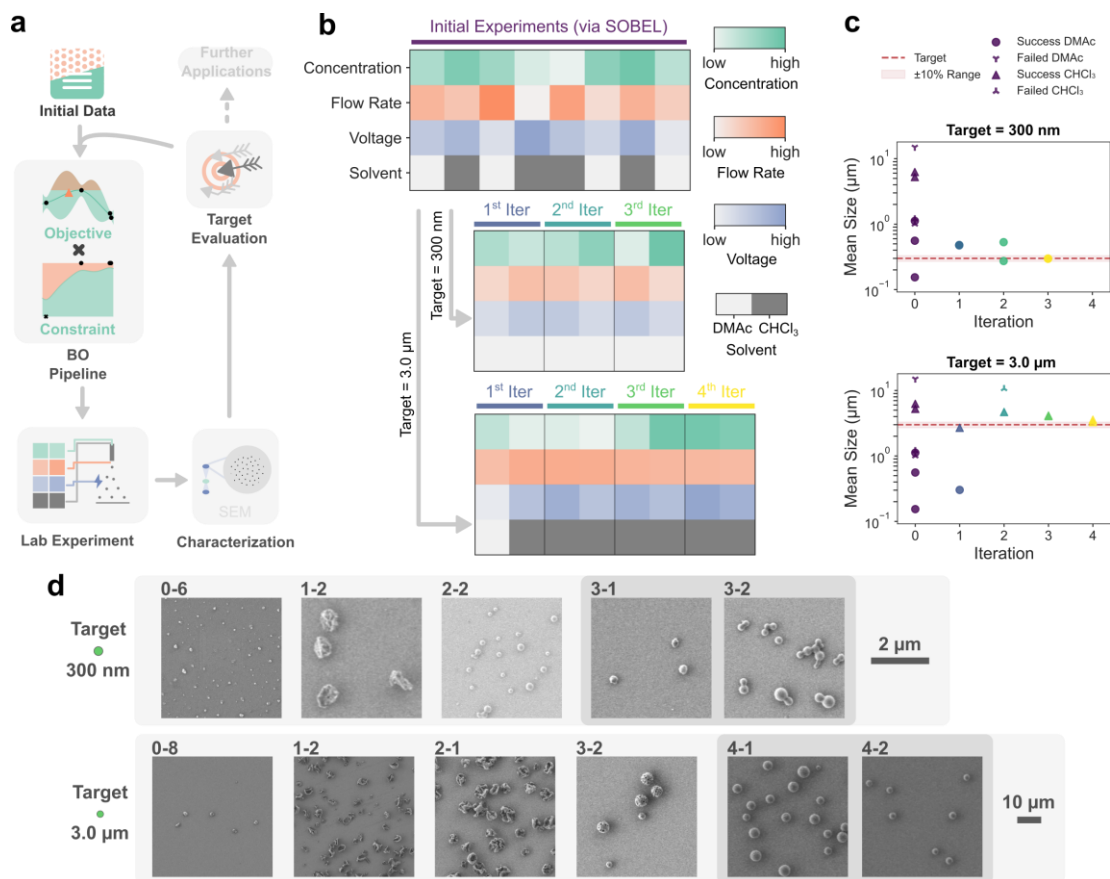


Fig. 2. Guiding electrospray experiments with CCBO. **a** A schematic diagram representing the experiment process with integration of CCBO. **b** Heatmaps visualizing the processing parameters used for (top) initial experiments, (middle) 300 nm target, and (bottom) 3.0 μm target. The initial experiments were generated with Sobel sequence and the targeted experiment series were suggested by CCBO pipeline. **c** Experiment results of particles generated with electrospraying under parameters proposed for (top) 300 nm and (bottom) 3.0 μm target. Each data point represents the mean of triplicated laboratory experiments. Symbols represent the solvent used and feasibility of experiment. **d** SEM images of particles produced at different iterations for (top) 300 nm and (bottom) 3.0 μm target.

Discussion

The present work demonstrated the application of efficient CCBO pipeline for target value optimization under black-box constraints. The two compartments in CCBO worked cohesively to address the need for guiding particle synthesis. For target optimization, the composite BO demonstrated strong capacity in modeling under the composited distance function over the underlying, black-boxed electrospray relationship function. On the other hand, the constraint compartment managed to learn and regulate the suggested experiments with a variational Gaussian process. To deal with unknown feasibility boundaries, many current strategies chose to apply active learning for the identification of unknown feasibility regions, followed by

running BO pipelines under the established boundaries^{30,31}. As an improvement, CCBO was designed for integrating these two individual processes and focus on identifying the feasibility regions around the design target. This could be seen from the initial experiments where the infeasibility caused by the mismatching of high flow rate with a less volatile solvent DMAc (experiment 0-3 on **Supplementary Table 1**) was not further explored because the target only requires experiments in the lower flow rate region. In comparison, with an active learning pipeline, extra experiments would be needed to determine the possible range for DMAc. Thus, the design of CCBO pipeline allows efficient reduction in the number of experiments to save laboratory resources.

In addition, the innate exploration-exploitation trade-off from BO made possible the identification of multiple possible experimental parameters that can achieve the same design target. This is especially helpful when other design considerations coexist. For example, in the validation with the synthetic problem (**Fig. 1f**), CCBO attempted both DMAc and chloroform and paired them with a wide range of other processing parameters to hit the design target in iterations 6 to 10. From the perspective of production rate, a higher flow rate and polymer concentration might be preferred. Similarly, if the sustainability of the solvent is considered, DMAc would be selected over chloroform as a less harsh solvent. On top of the synthetic data, laboratory experiments also managed to find multiple parameters to produce particles with 300 nm or 3.0 μm diameter. These particles exhibited distinctive morphology and polydispersity, demonstrating varying characteristics for their applications. Although not explicitly coded as a multiple-objective optimization problem, these sets of experimental parameters could be presented to the user as alternative choices. In practice, such flexibility allows the researcher to consider product properties, manufacturing metrics, or other aspects in production, without changing the main design target.

Notably, we highlight that the CCBO pipeline can be seamlessly extended to a broader range of processing parameters, such as involving a wider range of solvents through expanding the boundaries conditions at each iteration. Furthermore, CCBO could potentially be extended to other particle synthesis systems, such as batch methods and microfluidics, to facilitate the guided design and production of particles. In the past, the resource-demanding nature of experimentation and scarcity of data posed significant challenges and prolonged the workflow of particle synthesis. We are expecting CCBO to empower nanotechnology with a smarter and more efficient paradigm for target-driven design.

Methods

Constrained composite Bayesian optimization. Two components were incorporated in the BO pipeline and were developed under the framework of BoTorch³² and GPyTorch³³. The objective component, which tracked the distance (or particle size in the case of CCBO), followed the classical design of BO (see **Supplementary Note 1** for details of handling categorical inputs)¹². Notably, due to the difficulty in determining the noise level in experiments, we assumed the input data from laboratory experiments, after averaging over triplicates, to be noiseless. In terms of the acquisition function, q -Expected Improvement (q EI, or batch EI) as a thoroughly investigated strategy was selected to allow consideration of multiple candidates jointly in each iteration. In its simplistic form where q equals 1, EI acquisition function at a single point x_0 can be given by $\alpha_{EI}(x_0) = \mathbb{E}[\max(y_0 - f^*, 0)]$, where $y_0 \sim \mathcal{N}(\mu(x_0), \sigma^2(x_0))$ with $\mu(x_0)$ and $\sigma^2(x_0)$ being the posterior mean and variance from the Gaussian process at x_0 , g^* is the current best observation. As the calculation of expectation requires integrating over the posterior, it becomes analytically intractable under a batched scenario where $q > 1$. We followed the strategy in BoTorch where Monte-Carlo sampling was used to approximate the expectation by:

$$\alpha_{qEI}(X) \approx \frac{1}{N} \sum_{i=1}^N \max_{j=1, \dots, q} [\max(y_{o,ij} - g^*, 0)], y_{o,ij} \sim \mathbb{P}(GP(X) | \mathcal{D}) \quad (1)$$

where N was the total number of Monte-Carlo sampling, q was the number of candidates to be evaluated jointly, and $y_{o,ij}$ was sampled through the reparameterization trick from the Gaussian process conditioned on data \mathcal{D} . Notably, the data \mathcal{D} consisted of $\{(x_i, y_{o,i})\}_{i=1}^n$ where $y_o = g(s) = -(s - s_o)^2$ with s_o representing the target size. g^* in the acquisition function represents the current minimum distance achieved. Under such configurations, this vanilla BO pipeline could help identify suitable experiment variables X that can maximize this negative distance measure y_o .

Furthermore, the second feasibility component was introduced to learn black-box constraints in the experiment. Here, a variational Gaussian process was implemented for the binary classification of experimental success or failure³³. The details for variational inference for Gaussian classification were described in previous publications³⁴. Briefly, the latent Gaussian process is further wrapped with a Probit regression to limit the output between 0 and 1, for the purpose of approximating a Bernoulli posterior. For our latent Gaussian process, it followed the same constant mean prior and kernel functions to incorporate mixed inputs. To incorporate feasibility modelling in the Bayesian optimization process, we extracted the posterior probability as a scaling factor in the acquisition function: $\alpha_{qEI\text{con}}(X) = \mathbb{P}(y_c = 1 | X) *$

$\alpha_{\text{qEI}}(X)$. Incorporating this factor in the acquisition function allowed the suppression of the value of experiments that are potentially infeasible, creating our constrained BO pipeline.

Both the vanilla and constrained BO pipelines had the Gaussian process modeling y_o and attempted to minimize this distance. As a different strategy, composite BO used a Gaussian process to directly model the particle size s . The composite part, namely the negative squared distance function g , was separated from the input data. Instead, the distance function was directly applied to the Gaussian posterior in the acquisition function:

$$\alpha_{\text{qEICF}}(X) \approx \frac{1}{N} \sum_{i=1}^N \max_{j=1, \dots, q} [\max(g(s_{ij}) - g^*, 0)], s_{ij} \sim \mathbb{P}(GP(X) | \mathcal{D}') \quad (2)$$

where s_{ij} was sampled through the reparameterization trick and $\mathcal{D}' = \{(x_i, s_i)\}_{i=1}^n$. When coupling the composite acquisition function α_{qEICF} with the constraint probability, we have the acquisition function for CCBO: $\alpha_{\text{qEICFcon}}(X) = \mathbb{P}(y_c = 1 | X) * \alpha_{\text{qEICF}}(X)$.

In the present work, the Monte-Carlo sampling number N was 512 and q was fixed to 2 throughout all BO pipelines. All input X were normalized to unit cubes, and the flow rate variable was transformed to logarithm before normalization. The outcomes of the objective component, including the distance variable, y_{obj} , in vanilla BO and constrained BO, as well as the particle size variable, s , in CCBO, were standardized to zero mean and unit variance. The outcomes of the feasibility component, y_c , were rescaled to $\{-1, 1\}$.

Synthetic electrospray data generation. The synthetic data of electrospray was generated through the following functions:

$$s = 2 * \frac{(Qc)^{\frac{1}{2}}}{\log(U)} + \alpha + 0.4 \quad (3)$$

$$y_{con} = \begin{cases} 1, & \text{if } \log(Q) * \alpha + 1.4 > 0 \\ 0, & \text{otherwise.} \end{cases} \quad (4)$$

where s is the particle size (μm), Q is the flow rate ($\mu\text{L}/\text{min}$), c is the concentration of the polymer solution (% w/v), U is the applied voltage (kV). The α is a constant depending on the solvent (CHCl_3 : 1, DMAc : 0).

Validating BO with synthetic data. The targeting particle size s_o was arbitrarily set to be 0.6, 3.0, 6.0 and 18.0 μm to validate BO performance. In each run, three BO pipelines and the random baseline were performed for 10 iterations with the starting data listed on **Table 2**. The outcomes of experiments were calculated by synthetic **equations (3) and (4)** from the corresponding experimental variables. Each run was repeated 20 times to account for variations. The regret, defined by the closest distance towards the targeting particle size, was plotted in

each iteration. The experimental variables proposed in a typical run were visualized on 3D plots with symbols representing solvent and feasibility, and colors encoding the iteration.

Table 2. Boundaries of Experiment Variables for BO and the Starting Data for Synthetic Experiments.

Label	Polymer Concentration (%) w/v)	Flow Rate ($\mu\text{L}/\text{min}$)	Voltage (kV)	Solvent
Bounds	[0.05-5.00]	[0.01-60.00]	[10.0-18.0]	{CHCl ₃ , DMAc}
S-1	0.50	15.00	10.0	DMAc
S-2	0.50	0.10	10.0	CHCl ₃
S-3	3.00	20.00	15.0	DMAc
S-4	1.00	20.00	10.0	CHCl ₃
S-5	0.20	0.02	10.0	CHCl ₃

Guiding laboratory experiments with CCBO. The boundaries of experimental variables remained the same as the validation with synthetic data. The starting eight experiments were generated through a Sobel sequence within boundaries for each variable. The targeted particle sizes were 300 nm and 3.0 μm based on domain expertise in drug delivery. The two experiments in each iteration were performed in triplicates. The results were fed back to the BO pipeline to obtain the next recommendations. The stopping criterion was set as achieving $\pm 10\%$ to the targeting size.

Materials. PLGA (PURASORB PDLG 5004A, 50:50 ratio) was purchased from Corbion (Amsterdam, The Netherlands). Chloroform and N, N-Dimethylacetamide (DMAc) were purchased from Sigma-Aldrich (Gillingham, UK).

Electrospraying production of particles. PLGA solutions were prepared by mixing PLGA granules with solvents at ambient temperature with magnetic stirring overnight. The solutions were fed by a syringe pump (Harvard PHD Ultra, Edenbridge, UK) to a 22-gauge needle (outer diameter 0.71 mm) through a capillary. The positive output of a high voltage power supply (Glassman High Voltage Inc., NJ, United States) was connected to the needle through a crocodile clamp and the collection plate was connected to the ground. Before electrospraying, the flow rate and voltage were adjusted to the values recommended by BO. Experiments were conducted at atmospheric pressure. The temperature and humidity in the room were controlled to be 19-22 $^{\circ}\text{C}$ and 40-50%. Particles were collected on a glass slide placed on the collection plate for Scanning Electron Microscopy (SEM) analysis. Zeiss Gemini 360 SEM (Germany) was used under an acceleration voltage of 1.0 kV with an SE2 detector. For each sample, three images were taken randomly at different locations. Images were further analyzed using ImageJ (National Institute of Health, USA). To obtain mean particle size, a hundred particles were

randomly measured for their diameters. For infeasible experiments, the diameters of splashes from undried droplets on the collecting glass slides were recorded as a measurement of size.

Data availability

Benchmark data in support of this study is available at <https://github.com/FrankWanger/CCBO.git>. The raw experiment data is available on request.

Code availability

The code required for reproducing the benchmark results, including the implementation of vanilla BO, constrained BO, and CCBO, are available at <https://github.com/FrankWanger/CCBO.git>.

Reference

1. Mitchell, M. J. *et al.* Engineering precision nanoparticles for drug delivery. *Nat. Rev. Drug Discov.* **20**, 101–124 (2021).
2. Stuart, M. A. C. *et al.* Emerging applications of stimuli-responsive polymer materials. *Nat. Mater.* **9**, 101–113 (2010).
3. Colombo, S. *et al.* Transforming nanomedicine manufacturing toward Quality by Design and microfluidics. *Adv. Drug Deliv. Rev.* **128**, 115–131 (2018).
4. Poon, W., Kingston, B. R., Ouyang, B., Ngo, W. & Chan, W. C. W. A framework for designing delivery systems. *Nat. Nanotechnol.* **15**, 819–829 (2020).
5. Rao, L., Yuan, Y., Shen, X., Yu, G. & Chen, X. Designing nanotheranostics with machine learning. *Nat. Nanotechnol.* 1–13 (2024) doi:10.1038/s41565-024-01753-8.
6. Tao, H. *et al.* Nanoparticle synthesis assisted by machine learning. *Nat. Rev. Mater.* **6**, 701–716 (2021).
7. Antony, J. *Design of Experiments for Engineers and Scientists*. (Elsevier, London, 2014).
8. Batra, R., Song, L. & Ramprasad, R. Emerging materials intelligence ecosystems propelled by machine learning. *Nat. Rev. Mater.* (2020) doi:10.1038/s41578-020-00255-y.
9. Xu, P., Ji, X., Li, M. & Lu, W. Small data machine learning in materials science. *Npj Comput. Mater.* **9**, 1–15 (2023).
10. Greenhill, S., Rana, S., Gupta, S., Vellanki, P. & Venkatesh, S. Bayesian Optimization for Adaptive Experimental Design: A Review. *IEEE Access* **8**, 13937–13948 (2020).
11. Rasmussen, C. E. & Williams, C. K. I. *Gaussian Processes for Machine Learning*. (MIT Press, Cambridge, Mass., 2008).
12. Shields, B. J. *et al.* Bayesian reaction optimization as a tool for chemical synthesis. *Nature* **590**, 89–96 (2021).
13. Szymanski, N. J. *et al.* An autonomous laboratory for the accelerated synthesis of novel materials. *Nature* **624**, 86–91 (2023).
14. Lookman, T., Balachandran, P. V., Xue, D. & Yuan, R. Active learning in materials science with emphasis on adaptive sampling using uncertainties for targeted design. *Npj Comput. Mater.* **5**, 1–17 (2019).
15. Jones, D. R., Schonlau, M. & Welch, W. J. Efficient Global Optimization of Expensive Black-Box Functions. *J. Glob. Optim.* **13**, 455–492 (1998).

16. Hoffer, J. G., Ranftl, S. & Geiger, B. C. Robust Bayesian target value optimization. *Comput. Ind. Eng.* **180**, 109279 (2023).
17. Borkowski, O. *et al.* Large scale active-learning-guided exploration for in vitro protein production optimization. *Nat. Commun.* **11**, 1872 (2020).
18. Ortiz-Perez, A., Van Tilborg, D., Van Der Meel, R., Grisoni, F. & Albertazzi, L. Machine learning-guided high throughput nanoparticle design. *Digit. Discov.* **3**, 1280–1291 (2024).
19. Gardner, J. R., Kusner, M. J., Xu, Z., Weinberger, K. Q. & Cunningham, J. P. Bayesian optimization with inequality constraints. in *Proceedings of the 31st International Conference on International Conference on Machine Learning - Volume 32 II-937-II-945* (JMLR.org, Beijing, China, 2014).
20. J. Hickman, R., Aldeghi, M., Häse, F. & Aspuru-Guzik, A. Bayesian optimization with known experimental and design constraints for chemistry applications. *Digit. Discov.* **1**, 732–744 (2022).
21. Ali, A. *et al.* Electrohydrodynamic atomisation driven design and engineering of opportunistic particulate systems for applications in drug delivery, therapeutics and pharmaceuticals. *Adv. Drug Deliv. Rev.* **176**, 113788 (2021).
22. Xie, J., Jiang, J., Davoodi, P., Srinivasan, M. P. & Wang, C.-H. Electrohydrodynamic atomization: A two-decade effort to produce and process micro-/nanoparticulate materials. *Chem. Eng. Sci.* **125**, 32–57 (2015).
23. Zhang, H. B., Edirisinghe, M. J. & Jayasinghe, S. N. Flow behaviour of dielectric liquids in an electric field. *J. Fluid Mech.* **558**, 103–111 (2006).
24. Astudillo, R. & Frazier, P. I. Thinking Inside the Box: A Tutorial on Grey-Box Bayesian Optimization. in *2021 Winter Simulation Conference (WSC)* 1–15 (IEEE, Phoenix, AZ, USA, 2021). doi:10.1109/WSC52266.2021.9715343.
25. Astudillo, R. & Frazier, P. Bayesian Optimization of Composite Functions. in *Proceedings of the 36th International Conference on Machine Learning* 354–363 (PMLR, 2019).
26. Wang, F. *et al.* Machine learning predicts electrospray particle size. *Mater. Des.* **219**, 110735 (2022).
27. Parhizkar, M. *et al.* Performance of novel high throughput multi electrospray systems for forming of polymeric micro/nanoparticles. *Mater. Des.* **126**, 73–84 (2017).
28. Hartman, R. P. A., Brunner, D. J., Camelot, D. M. A., Marijnissen, J. C. M. & Scarlett, B. JET BREAK-UP IN ELECTROHYDRODYNAMIC ATOMIZATION IN THE CONE-JET MODE. *J. Aerosol Sci.* **31**, 65–95 (2000).
29. Xu, J. *et al.* Studies on preparation and formation mechanism of poly(lactide-co-glycolide) microrods via one-step electrospray and an application for drug delivery system. *Eur. Polym. J.* **148**, 110372 (2021).
30. Khatamsaz, D. *et al.* Bayesian optimization with active learning of design constraints using an entropy-based approach. *Npj Comput. Mater.* **9**, 1–14 (2023).
31. Arróyave, R. *et al.* A perspective on Bayesian methods applied to materials discovery and design. *MRS Commun.* **12**, 1037–1049 (2022).
32. Balandat, M. *et al.* BOTORCH: a framework for efficient monte-carlo Bayesian optimization. in *Proceedings of the 34th International Conference on Neural Information Processing Systems* 21524–21538 (Curran Associates Inc., Red Hook, NY, USA, 2020).
33. Gardner, J. R., Pleiss, G., Bindel, D., Weinberger, K. Q. & Wilson, A. G. GPyTorch: blackbox matrix-matrix Gaussian process inference with GPU acceleration. in *Proceedings of the 32nd International Conference on Neural Information Processing Systems* 7587–7597 (Curran Associates Inc., Red Hook, NY, USA, 2018).

34. Hensman, J., Matthews, A. & Ghahramani, Z. Scalable Variational Gaussian Process Classification. in *Proceedings of the Eighteenth International Conference on Artificial Intelligence and Statistics* 351–360 (PMLR, San Diego, California, USA, 2015).

Acknowledgements

The author Fanjin Wang would like to thank the Engineering and Physical Sciences Research Council (EPSRC) for supporting his PhD research (EP/R513143/1 and EP/W524335/1). Dr Jakob Zeitler from Matterhorn Studio is thanked for initial discussions. Ms Scheilly Tsilova and Ms Amenah Al-barudi from University College London are gratefully acknowledged for providing their expertise in the human vs. BO comparison.

Author contributions

F.W. conceptualized the study, developed methodology and software, and performed investigation. M.P. and A.H. helped with methodology. M.P. and M.E. provided resources and supervision. F.W. drafted the original manuscript. M.P., A.H., and M.E. edited and revised the manuscript. All authors approved the final version.

Competing interests

The authors declare no competing interests.

Supplementary information for

Constrained composite Bayesian optimization for rational synthesis of polymeric particles

Fanjin Wang^{1,2,*}, Maryam Parhizkar², Anthony Harker³, Mohan Edirisinghe¹

¹Department of Mechanical Engineering, University College London, London, WC1E 7JE, United Kingdom

²School of Pharmacy, University College London, London, WC1N 1AX, United Kingdom

³Department of Physics and Astronomy, University College London, London, WC1E 6BT, United Kingdom

*Corresponding author, email: fanjin.wang.20@ucl.ac.uk

Supplementary Notes

Supplementary Note 1: Surrogate development for CCBO and baseline BO methods.

A Gaussian process with constant mean prior was used as the surrogate function¹. As the input consists of both continuous (i.e., processing parameters) and categorical (solvents) variables, the covariance module of the Gaussian process adopted the design in BoTorch² to combine the categorical and a continuous kernel. More specifically, the mixed kernel was defined by:

$$\begin{aligned} k_{\text{Mixed}}\left(\left(\mathbf{x}_{c,1}, \mathbf{x}_{d,1}\right), \left(\mathbf{x}_{c,2}, \mathbf{x}_{d,2}\right)\right) \\ = k_{\text{Matérn52}}\left(\mathbf{x}_{c,1}, \mathbf{x}_{c,2}\right) + k_{\text{Hamming}}\left(\mathbf{x}_{d,1}, \mathbf{x}_{d,2}\right) \\ + k_{\text{Matérn52}}\left(\mathbf{x}_{c,1}, \mathbf{x}_{c,2}\right) * k_{\text{Hamming}}\left(\mathbf{x}_{d,1}, \mathbf{x}_{d,2}\right), \end{aligned} \quad (1)$$

where \mathbf{x}_c and \mathbf{x}_d were the continuous and discrete compartments in the input, respectively. The $k_{\text{Matérn52}}$ was a Matérn kernel with the smoothness parameter ν set as $5/2$:

$$k_{\text{Matérn52}}\left(\mathbf{x}_{c,1}, \mathbf{x}_{c,2}\right) = \frac{2^{1-\nu}}{\Gamma(\nu)} \left(\sqrt{2\nu}d\right)^\nu K_\nu\left(\sqrt{2\nu}d\right), \quad (2)$$

where $d = \left(\mathbf{x}_{c,1} - \mathbf{x}_{c,2}\right)^\top \Theta \left(\mathbf{x}_{c,1} - \mathbf{x}_{c,2}\right)$ with Θ being the length scale parameter, Γ was the gamma function, and K_ν was a modified Bessel function. The k_{Hamming} was a categorical kernel based on Hamming distance:

$$k_{\text{Hamming}}\left(\mathbf{x}_{d,1}, \mathbf{x}_{d,2}\right) = e^{-\frac{HD\left(\mathbf{x}_{d,1}, \mathbf{x}_{d,2}\right)}{\Theta}}, \quad (3)$$

where HD was the Hamming distance function.

Supplementary Tables:

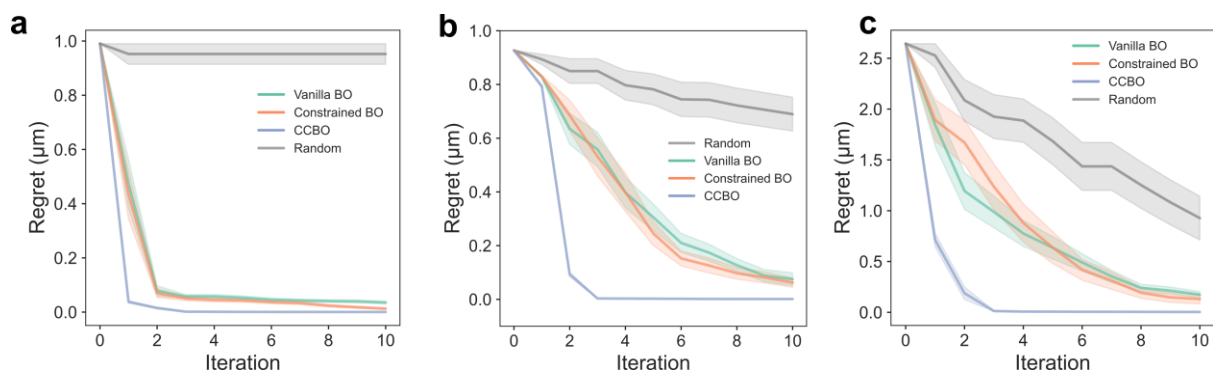
Supplementary Table 1. Processing parameters generated through CCBO for target 300 nm and the resulting particle sizes and feasibility (N=3).

Label	Polymer Concentration (% w/v)	Flow Rate ($\mu\text{L}/\text{min}$)	Voltage (kV)	Solvent	Mean Size (μm)	Feasible?
1-1	2.32	0.09	12.0	DMAc	0.48	1
1-2	1.33	0.74	13.9	DMAc	0.47	1
2-1	1.89	0.43	13.9	DMAc	0.53	1
2-2	3.52	0.10	12.3	DMAc	0.27	1
3-1	0.58	0.84	14.0	DMAc	0.30	1
3-2	4.61	0.07	12.4	DMAc	0.30	1

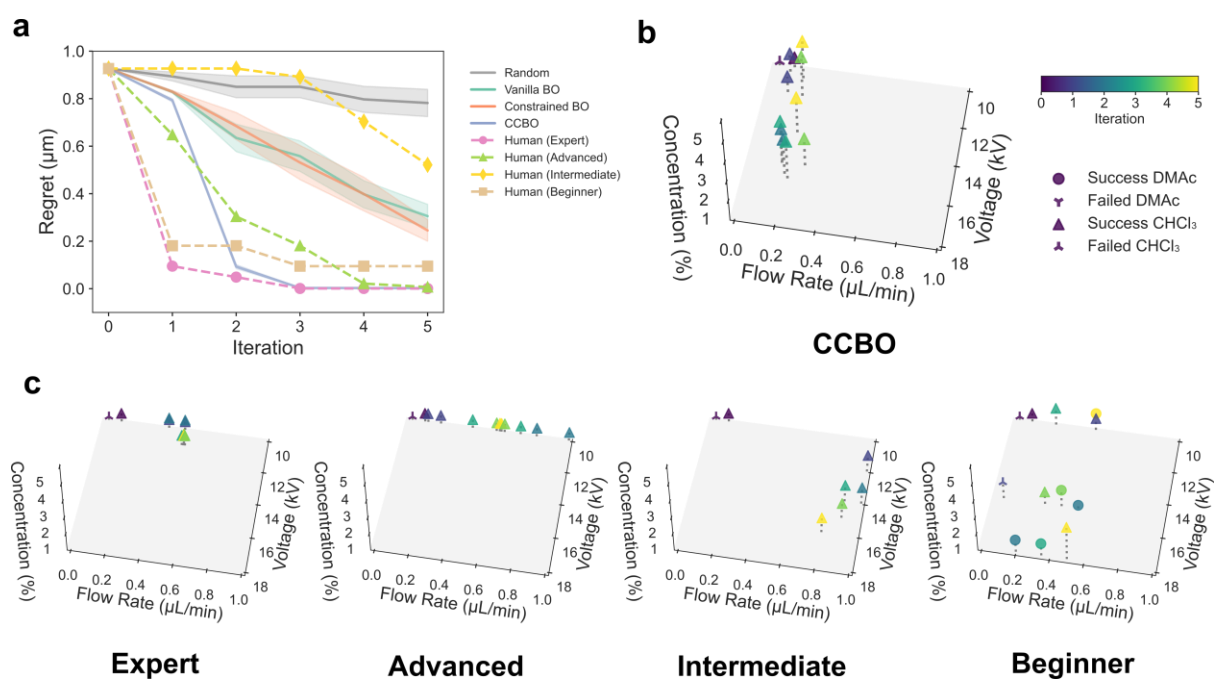
Supplementary Table 2. Processing parameters generated through CCBO for target 3.0 μm and the resulting particle sizes and feasibility (N=3).

Label	Polymer Concentration (% w/v)	Flow Rate ($\mu\text{L}/\text{min}$)	Voltage (kV)	Solvent	Mean Size (μm)	Feasible?
1-1	1.66	0.80	10.7	DMAc	0.30	1
1-2	0.36	3.65	14.6	CHCl_3	2.69	1
2-1	0.57	3.74	16.5	CHCl_3	4.69	1
2-2	0.05	3.55	14.5	CHCl_3	10.64	0
3-1	1.63	1.92	16.2	CHCl_3	4.14	1
3-2	4.51	1.38	14.9	CHCl_3	4.05	1
4-1	4.45	1.30	17.4	CHCl_3	3.58	1
4-2	4.02	1.08	16.3	CHCl_3	3.29	1

Supplementary Figures:



Supplementary Figure 1. Benchmark results with random baseline, vanilla BO, constrained only BO, and CCBO for **a** 0.6 μm , **b** 3.0 μm and **c** 6.0 μm targets. Each benchmark experiment was performed for 10 iterations. Shaded areas indicate standard error from 20 times repetition.



Supplementary Figure 2. **a** Benchmark results of target value optimization for 3.0 μm target in comparison with human users. Each benchmark experiment was performed for 5 iterations. Shaded areas indicate standard error from 20 times repetition. **b** Visualization of experiments selected by the CCBO pipeline. **c** Visualization of experiments selected by human users with various experience levels. Each data point represents one ‘synthetic’ experiment. The corresponding iteration is coded by color. Symbols represent the solvent used and feasibility of experiment.

Supplementary References

1. Shields, B. J. *et al.* Bayesian reaction optimization as a tool for chemical synthesis. *Nature* **590**, 89–96 (2021).
2. Balandat, M. *et al.* BOTORCH: a framework for efficient monte-carlo Bayesian optimization. in *Proceedings of the 34th International Conference on Neural Information Processing Systems* 21524–21538 (Curran Associates Inc., Red Hook, NY, USA, 2020).